

SANDIA REPORT

SAND2013-7824

Unlimited Release

Printed September 2013

3D Deformation Field Throughout the Interior of Materials

Helena Jin, Wei-Yang Lu

Prepared by
Sandia National Laboratories
Albuquerque, New Mexico 87185 and Livermore, California 94550

Sandia National Laboratories is a multi-program laboratory managed and operated by Sandia Corporation, a wholly owned subsidiary of Lockheed Martin Corporation, for the U.S. Department of Energy's National Nuclear Security Administration under contract DE-AC04-94AL85000.

Approved for public release; further dissemination unlimited.



Sandia National Laboratories

Issued by Sandia National Laboratories, operated for the United States Department of Energy by Sandia Corporation.

NOTICE: This report was prepared as an account of work sponsored by an agency of the United States Government. Neither the United States Government, nor any agency thereof, nor any of their employees, nor any of their contractors, subcontractors, or their employees, make any warranty, express or implied, or assume any legal liability or responsibility for the accuracy, completeness, or usefulness of any information, apparatus, product, or process disclosed, or represent that its use would not infringe privately owned rights. Reference herein to any specific commercial product, process, or service by trade name, trademark, manufacturer, or otherwise, does not necessarily constitute or imply its endorsement, recommendation, or favoring by the United States Government, any agency thereof, or any of their contractors or subcontractors. The views and opinions expressed herein do not necessarily state or reflect those of the United States Government, any agency thereof, or any of their contractors.

Printed in the United States of America. This report has been reproduced directly from the best available copy.

Available to DOE and DOE contractors from
U.S. Department of Energy
Office of Scientific and Technical Information
P.O. Box 62
Oak Ridge, TN 37831

Telephone: (865) 576-8401
Facsimile: (865) 576-5728
E-Mail: reports@adonis.osti.gov
Online ordering: <http://www.osti.gov/bridge>

Available to the public from
U.S. Department of Commerce
National Technical Information Service
5285 Port Royal Rd.
Springfield, VA 22161

Telephone: (800) 553-6847
Facsimile: (703) 605-6900
E-Mail: orders@ntis.fedworld.gov
Online order: <http://www.ntis.gov/help/ordermethods.asp?loc=7-4-0#online>



3D Deformation Field Throughout the Interior of Materials

Helena Jin, Wei-Yang Lu
Mechanics of Materials
Sandia National Laboratories
Livermore, CA 94550

Abstract

This report contains the one-year feasibility study for our three-year LDRD proposal that is aimed to develop an experimental technique to measure the 3D deformation fields inside a material body. In this feasibility study, we first apply Digital Volume Correlation (DVC) algorithm to pre-existing in-situ X-ray Computed Tomography (XCT) image sets with pure rigid body translation. The calculated displacement field has very large random errors and low precision that are unacceptable. Then we enhance these tomography images by setting threshold of the intensity of each slice. DVC algorithm is able to obtain accurate deformation fields from these enhanced image sets and the deformation fields are consistent with the global mechanical loading that is applied to the specimen. Through this study, we prove that the internal markers inside the pre-existing tomography images of aluminum alloy can be enhanced and are suitable for DVC to calculate the deformation field throughout the material body.

ACKNOWLEDGMENTS

We gratefully appreciate the support of the Advanced Light Source at Lawrence Berkeley National Laboratory, and in particular Alastair MacDowell and Dula Parkinson at the 8.3.2 tomography beamline for the acquisition of the tomographic images. We are thankful to Alejandro Mota, James Foulk and George Johnson for their contributions in reconstructing the tomography data. We also deeply appreciate the help from Hubert Schreier and Ning Li at Correlated Solutions, Inc.

This work was funded under LDRD Project Number 165661 and Title "3D Deformation Field Throughout the Interior of Materials".

CONTENTS

1. Introduction.....	9
1.1. Outline.....	9
2. In-situ XCT Experiments.....	11
3. Digital Volume Correlation (DVC).....	13
4. Study Cases of DVC Applications.....	15
4.1. Rigid Body Translation of XCT Slices in X-Y Plane.....	15
4.2. Enhancing the Image Set by Thresholding the Intensity	15
4.3. Calculation of Real Deformation Field from Tensile Testing	17
4.4. Imperfections in the DVC Results.....	19
5. Conclusions.....	21
6. References.....	23
Distribution.....	24

FIGURES

Figure 1. Schematic of an in-situ XCT Experiment	11
Figure 2: Stress~strain curve along transverse direction showing the loading steps for XCT imaging.	12
Figure 3: Reconstructed 3D images showing (a)-particles and (b)-voids at the initial stage, (c)-voids at loading step 4, (d)-voids at step 5, (e)-voids at step 6.....	12
Figure 4: DIC uses random speckle patterns to track the deformation on the surface	13
Figure 5: Principle of DVC	14
Figure 6: A typical XCT slice that will be used for DVC.....	14
Figure 7: XCT image set with rigid body translation in x-y plane. (a) Selected XCT slices from loading step 5; (b) Rigid body translation introduced in x-y plane.....	15
Figure 8: (a) Histogram of a typical XCT slice; (b) Magnified view of circled area in (a) showing the intensity of most voxels falls within	16
Figure 9: (a) Original image of a typical slice; (b) Rescaled image slice with enhanced features	16
Figure 10: DVC results from enhanced image set	17
Figure 11: (a) Selected volumes from scan #4 and #5 in Figure 7 are used as original and deformed image sets in DVC; (b) Subvolume with enhanced features for DVC.	18
Figure 12: Strain field ϵ_{zz} correlated from the selected volumes in Figure 11 are shown at different x-y planes.	18
Figure 13: Strain field ϵ_{zz} correlated from the selected volumes in Figure 11 shown at different x-z planes.	19

TABLES

Table 1. DVC Calculated Displacement Field for the Case of Simple Translation	15
Table 2: DVC Calculated Displacement Field from the Enhanced Image Set.....	17

NOMENCLATURE

XCT	X-ray Computed Tomography
DIC	Digital Image Correlation
DVC	Digital Volume Correlation
LBNL	Lawrence Berkeley National Laboratory
ESRF	European Synchrotron Radiation Facility
AOI	Area of Interest

1. INTRODUCTION

Recent advances in numerical simulation have enabled the availability of large quantities of full-field numerical data such as deformation throughout the whole material body. The ability to validate these numerical data, however, has been very limited. The obstacle lies in the difficulty of measuring 3D full-field deformation inside the material.

In the past, the conventional observation techniques, including optical and scanning electron microscopy, have been used to study the relationship between microstructure and mechanical behavior. These observation techniques, however, are limited to the surface, which may not represent the features inside. The sample preparation used for these techniques can also introduce artificial features that do not belong to the material. Recently, the spatial resolution of X-ray Computed Tomography (XCT) is decreased down to sub-micrometer, even nanometer scale, which has made XCT a very appealing tool to study the microstructures and material failure inside the material body. Digital Volume Correlation (DVC) is an emerging technique to quantify the deformation field inside an entire volume. Therefore, we propose to develop an experimental technique that couples powerful DVC algorithms with in-situ mechanical loading and XCT imaging to measure the full-field deformation inside a material body. In this work, we are applying DVC algorithm to the pre-existing tomography images of aluminum alloy to find out whether the internal features patterns in the tomography images are suitable for DVC to calculate the deformation field throughout the material body.

1.1. Outline

In section 2, we will briefly discuss the in-situ XCT experiments that we previously performed at LBNL and the acquisition and reconstruction of the tomography images of aluminum alloy. In section 3, we will introduce the full-field deformation techniques DIC and DVC and explain their principles. In section 4, we will examine a few application cases of DVC algorithm to the existing tomography data. In section 5, we will summarize our study results.

2. IN-SITU XCT EXPERIMENTS

X-ray Computed Tomography (XCT) is a very attractive 3D imaging technique which enables real 3D visualization of microstructure features inside a specimen. Previously, this technique is mainly limited to medical and biological applications due to its low spatial resolution. Recent advances in terms of resolution and portable light source availability have made the microXCT and nanoXCT a very valuable technique in the mechanics and materials research community [1]. There is recently an increasing amount of research aiming to characterize the internal damage and failure of various materials using XCT imaging combined with mechanical loading, especially from French researchers at European Synchrotron Radiation Facility (ESRF) [2-4].

Previously, we combined in-situ tensile loading and x-ray tomography to examine the internal microstructural damage evolution of aluminum alloy 7075-T7351 [5-6]. The in-situ XCT experiment was performed at the Advanced Light Source (ALS) at Lawrence Berkeley National Laboratory (LBNL). Figure 1 shows the schematic of in-situ XCT experiment. The specimen is mounted on a rotating stage located between the x-ray source and CCD detector. CCD detector records a radiograph of the projection of the material body when the x-ray transmits through it at each i^{th} incremental angular position. As the specimen rotates through 180° , N radiographs are recorded at different incremental angles. An angular increment of 0.125° is selected in this study, which results in $N=1440$ for the number of radiographs. A series of radiographs are acquired in-situ at each j^{th} incremental loading stage as the specimen is loaded step by step in front of x-ray. Here, M is the number of loading steps that are held steady for the XCT scan. The spatial resolution of XCT is $0.9 \mu\text{m}/\text{voxel}$. The voxel size of each projection is about 2500×1800 voxels², which is approximately equivalent to a projection area of $2.2\text{mm} \times 1.6\text{mm}$. The x-ray scan is performed in the middle of the specimen gage section, which is slightly tapered to make sure that the specimen would fail at the scanned area.

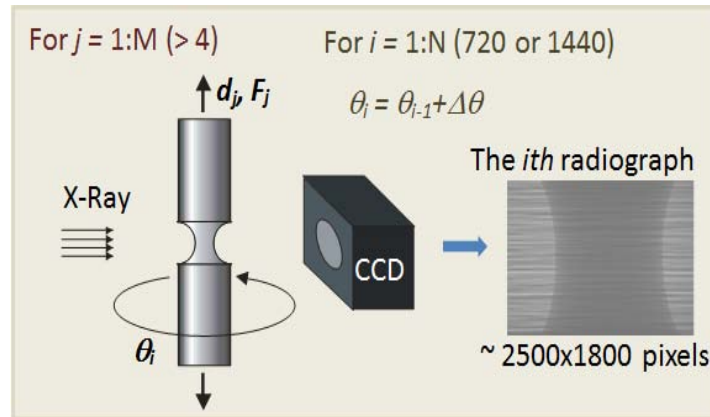


Figure 1. Schematic of an in-situ XCT Experiment

During the experiment, a series of radiographs corresponding to a large number of angular positions of the sample are recorded at selected incremental loading steps. Figure 2 shows a representative stress-strain curve for the specimen loaded along the transverse direction. The tomography scans are performed at selected loading steps as marked on the curve as: 1-

original unloaded state, 2-yield point, 3-hardening, 4-maximum load, 5-necking and 6-material failure.

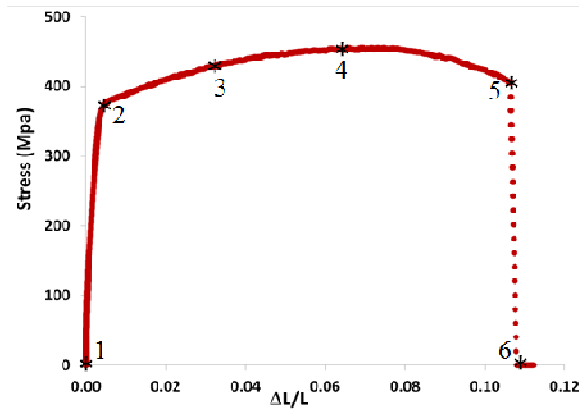


Figure 2: Stress~strain curve along transverse direction showing the loading steps for XCT imaging.

A reconstruction process is applied to the radiographs acquired at each loading step to obtain 3D digital images of the sample. The intensity of each voxel in the 3D image, which is the elementary unit of the 3D image, is defined by the linear x-ray attenuation coefficient of the material which is correlated to the density of the material at that location. The darker region in the 3D image is the material with lower density and the brighter region is the material with higher density. In the case of aluminum 7075, the intermetallic particles and voids inside the alloy matrix generate the intensity variation in the 3D image. The intermetallic particles correspond to the brighter region in the reconstructed 3D images and the voids correspond to the darker regions, as shown in Figures 3(a) and (b) for the initial loading step, Figure 3(c) is for loading step 4, 3(d) is for step 5 and Figure 3(e) is for loading step 6 in Figure 2. The gray color is corresponding to aluminum matrix.

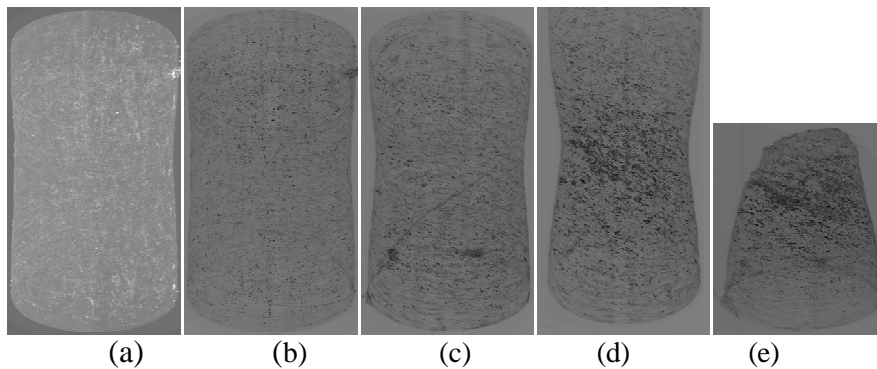


Figure 3: Reconstructed 3D images showing (a)-particles and (b)-voids at the initial stage, (c)-voids at loading step 4, (d)-voids at step 5, (e)-voids at step 6

3. DIGITAL VOLUME CORRELATION (DVC)

Digital image correlation (DIC) is a technique for full-field surface deformation measurement that mathematically compares a subset of a digital image from a reference configuration with a subset of a digital image from a deformed configuration. The DIC technique uses random speckle patterns on the surface of a specimen to track the deformation via comparison of the digitalized undeformed and deformed images, as shown in Figure 4. It is very critical to generate suitable patterns for DIC to obtain correct deformation results. In the case of speckle patterns on the specimen surface, we can either externally generate patterns using techniques such as spray painting, sputtering coating and lithography or use internal features such as topographic information on the surface, grain microstructures.

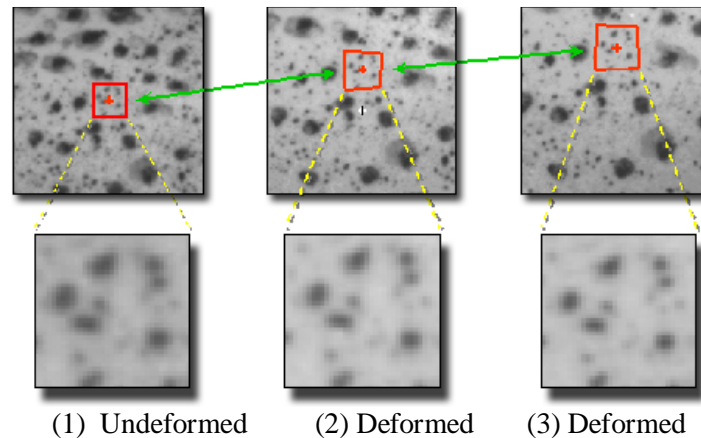


Figure 4: DIC uses random speckle patterns to track the deformation on the surface

With recent advances in 3D imaging capabilities and computing resources, the research interest in DVC has been increased significantly. Digital volume correlation (DVC) is an emerging technique that calculates the 3D deformation field of an entire volume by tracking the patterns/markers inside the 3D image. It is an extension of the 2D surface deformation measurement to 3D volumetric deformation measurement throughout the whole material body, as shown in Figure 5. Similar to DIC, DVC also requires appropriate pattern (or marker) density and distribution as well as sufficient image contrast. Contrary to surface speckles for DIC analysis, which can be generated or modified easily, the natural markers inside a material body that are used for DVC cannot be altered physically.

We have discussed in the previous section that the intermetallic particles and voids inside the aluminum alloy can generate the intensity variation and contrast in the tomographic image. However, the patterns from these internal features may be non-ideal and they cannot be physically modified. As you can see from a typical XCT slice shown in Figure 6, the image has low contrast and some of these internal features are sparse. Therefore, we aim to examine whether these internal features/markers are suitable for DVC to calculate the deformation inside the material body. We will discuss the results from several study cases in the following section.

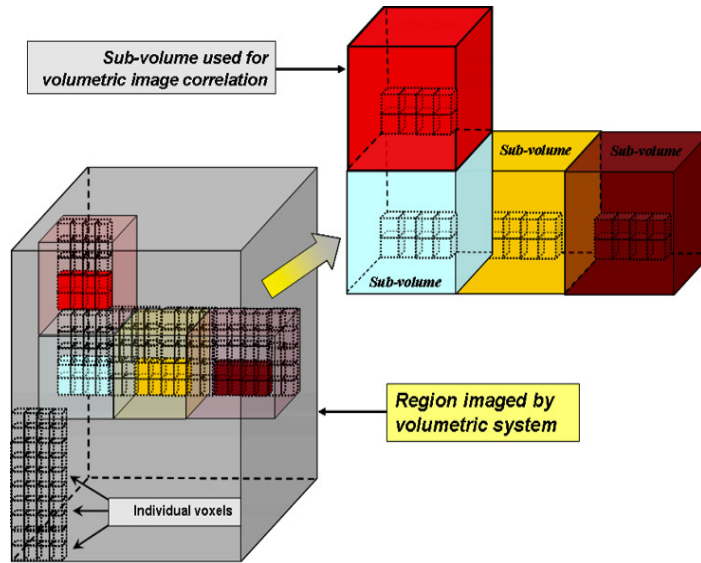


Figure 5: Principle of DVC

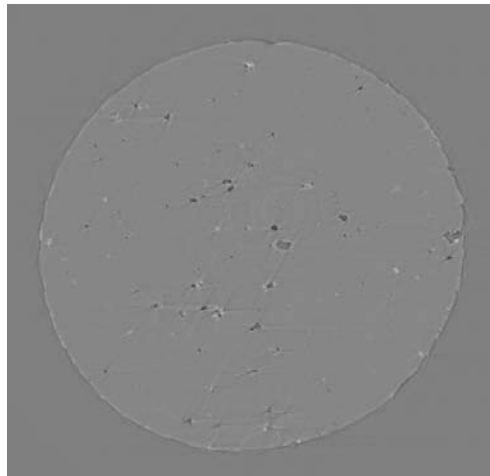


Figure 6: A typical XCT slice used for DVC

4. STUDY CASES OF DVC APPLICATIONS

4.1. Rigid Body Translation of XCT Slices in X-Y Plane

To quantify the accuracy of deformation field, we first apply DVC algorithm to the simple case of known rigid body translation. A set of XCT slices from loading step 5 are chosen as the original undeformed image set. The deformed image set is translated from the undeformed image set in x-y plane by 66 pixels in x-direction and 55 pixels in y-direction. The artificially introduced displacements are illustrated in Figure 7. An area of interest (AOI) 250×250 pixels² is selected through all the slices which create a volume of $250 \times 250 \times 200$ voxels³ for DVC to calculate the displacement field. We then conduct two tests with different subvolume sizes to examine how well DVC can perform the calculation. Test 1 has subvolume size of 23 and test 2 has subvolume size of 31. The step size for both tests is 11. Mean value of the displacement obtained from DVC is shown together with the ideal displacement value and standard deviation value in Table 1 (a) for test 1 and (b) for test 2. We can see that Test 2 has better results than test 1. However, the calculated displacement fields from both tests have very large standard deviation and the mean values are a few pixels off the actual value. Both tests have larger errors than typical correlation results, which should be normally within subvoxel. These results are unacceptable. Therefore, we need to investigate whether we can improve these XCT images to achieve better results.

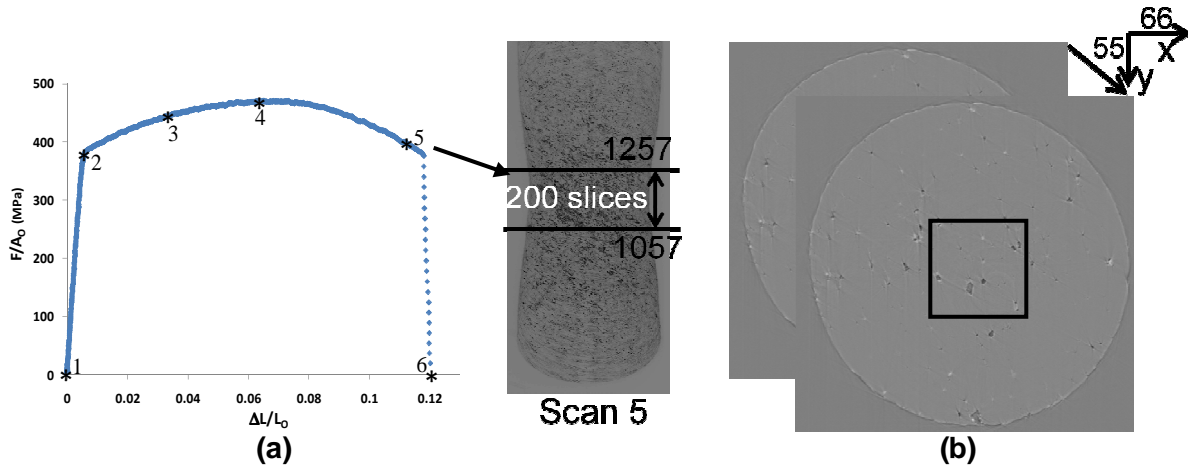


Figure 7: XCT image set with rigid body translation in x-y plane. (a) Selected XCT slices from loading step 5; (b) Rigid body translation introduced in x-y plane

Table 1. DVC Calculated Displacement Field for the Case of Simple Translation

	Test 1 (Subvolume size = 23)			Test 2 (Subvolume size = 31)		
	U	V	W	U	V	W
Applied Disp	66	55	0	66	55	0
Mean of Disp	60.5	49.2	3.1	65.2	53.4	1.2
Std of Disp	18.5	17.4	13.6	9.6	10.1	5.4

4.2. Enhancing the Image Set by Thresholding the Intensity

As we have discussed in Section 3, DVC relies on the internal pattern/marker inside the material to track 3D deformation throughout the material body. It requires image to have nice

contrast and wide distribution of the intensity. Figure 8(a) shows the gray level histogram from a typical XCT slice. We can clearly see that the distribution range of the gray level is very narrow. Figure 8(b) is a magnified view of circled area in (a) and we can see that the intensity of most voxels falls within $[\mu - 3\sigma, \mu + 3\sigma]$. To properly use the range of gray level to represent the variation in pattern, we threshold the intensity for all images: if intensity of a voxel is below $\mu - 3\sigma$, then it is set to $\mu - 3\sigma$; if intensity of a voxel is above $\mu + 3\sigma$, then it is set to $\mu + 3\sigma$. The original and the enhanced image are shown together in Figure 9(a) and (b). The features in the image are greatly enhanced by rescaling the intensity.

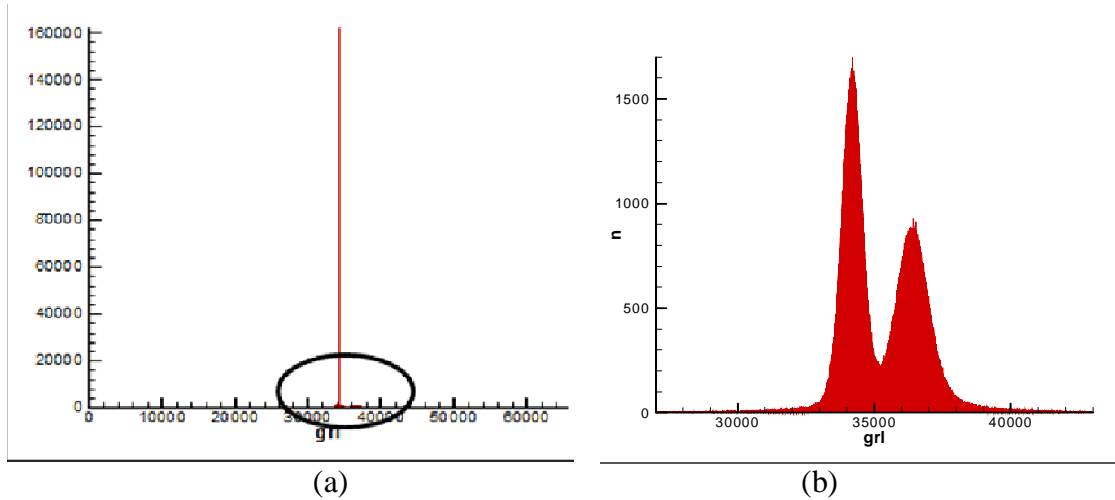


Figure 8: (a) Histogram of a typical XCT slice; (b) Magnified view of circled area in (a) showing the intensity of most voxels falls within $[\mu - 3\sigma, \mu + 3\sigma]$

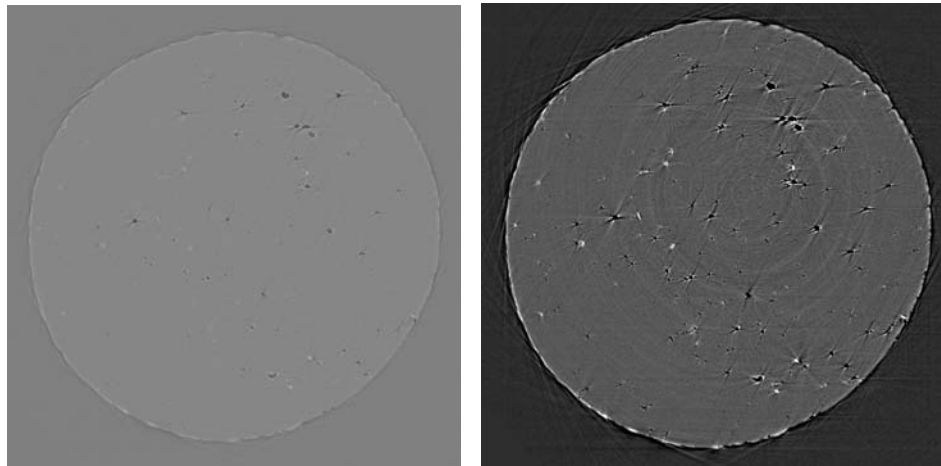


Figure 9: (a) Original image of a typical slice; (b) Rescaled image slice with enhanced features.

We now apply DVC to the enhanced image set with rigid body translation. First, a prior gross determination of displacement $U_{Prior} = [70, 50, 0]$ from direct comparison of the image set is used as initial guess. The total displacement is $U_{Tot} = U_{Prior} - U_{DVC}$. We use the same

DVC parameters as test 1 and the calculated DVC displacement U_{DVC} is $u = 4, v = -5, w = 0$. Then the total displacements are $U=66, V=55$ and $W=0$.

DVC results from these enhanced image sets are much more accurate and precise. Mean of DVC calculated displacement is same as the ideal displacement value and the standard deviation of the displacement is 0.001. DVC results from the enhanced image sets are shown in Figure 10. The mean and standard deviation of the displacement is shown in Table 2. We can clearly see that DVC is able to calculate the displacement fields from these rescaled image sets with enhanced features.

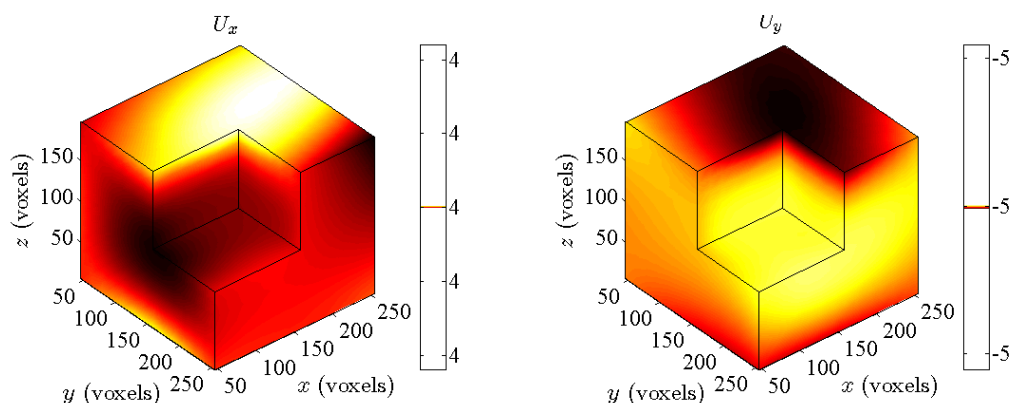


Figure 10: DVC results from enhanced image set

Table 2: DVC Calculated Displacement Field from the Enhanced Image Set

	U	V	W
Applied Disp	66	55	0
Mean of Disp	66.0	55.0	0
Std of Disp	0.001	0.000	0.001

4.3. Calculation of Real Deformation Field from Tensile Testing

It has now been demonstrated that DVC can be applied to the rescaled image set with enhanced features to calculate the displacement field for the simple case of rigid body translation. Next, we want to apply DVC to image sets with real deformation field from the in-situ XCT experiments. The application of DVC software to the image sets with real deformation is mainly conducted by Correlated Solutions Inc (CSI) through the contracted service. CSI has already developed the DVC software that works for some other applications. In this work, they need to optimize the DVC parameters and proper starting points to achieve best correlation results from these non-ideal tomography images.

As shown in Figure 7, an image set of 500 slices from scan 4 are selected as the original undeformed volume and an image set from scan 5 as the deformed volume. These two image sets are rescaled and improved as in section 4.2 by thresholding the intensity of all images so that the features inside are greatly enhanced to better suit for DVC calculation. Figure 11 shows the selection of original and deformed image sets and the subvolume with enhanced features. The calculated full-field strain ϵ_{zz} are shown in Figure 12 for different x-y planes and in Figure 13 for different x-z planes. We can clearly see that the strain field is smooth. The strain value varies

from 1% at the end of gage length to 11% in the middle of the gage section where the necking starts. The average strain is about 6%, which is consistent with the global strain applied between step #4 and #5. These strain fields calculated from DVC seem to be reasonable and consistent with global loading conditions. However, there are no other experimental techniques currently available to measure the displacement field inside the material body. Therefore, we cannot experimentally verify these results.

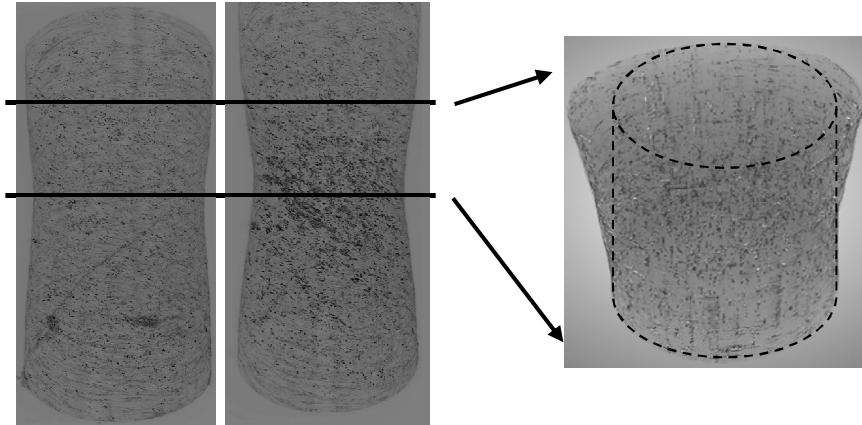


Figure 11: (a) Selected volumes from scan #4 and #5 in Figure 7 are used as original and deformed image sets in DVC; (b) Subvolume with enhanced features for DVC.

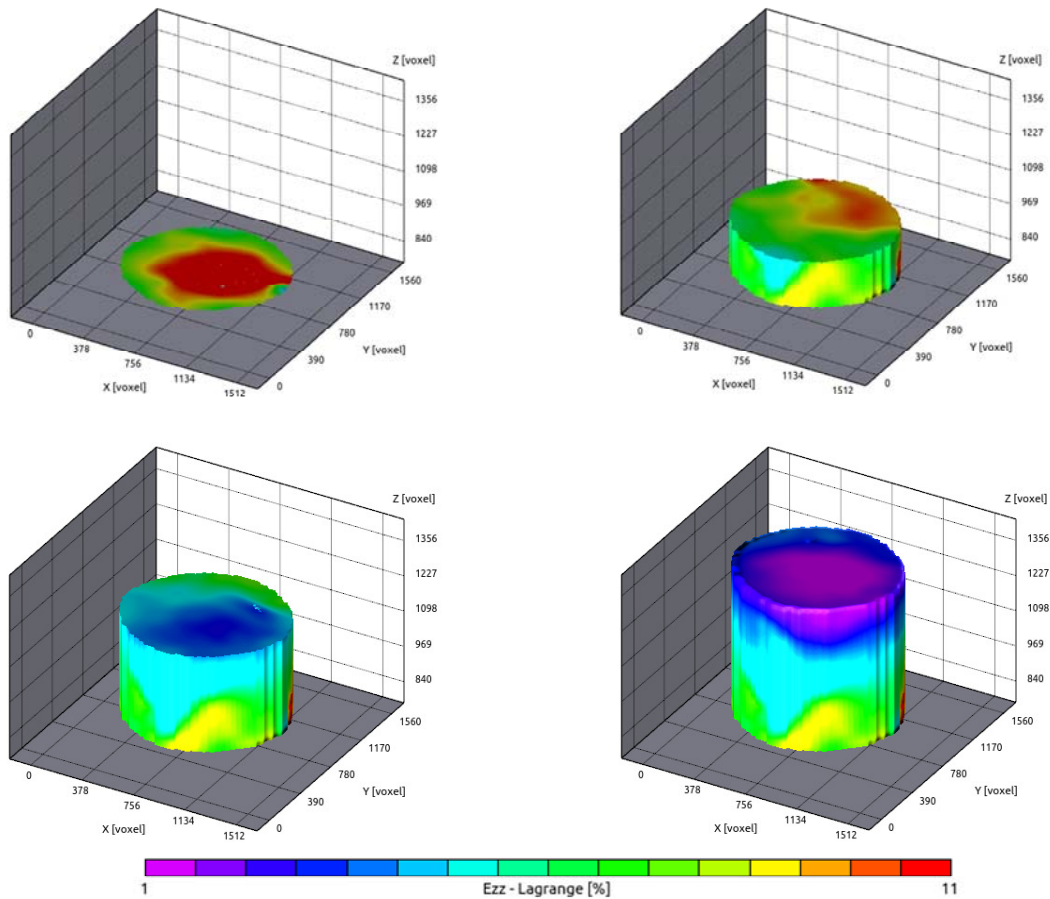


Figure 12: Strain field ϵ_{zz} correlated from the selected volumes in Figure 11 are shown at different x-y planes.

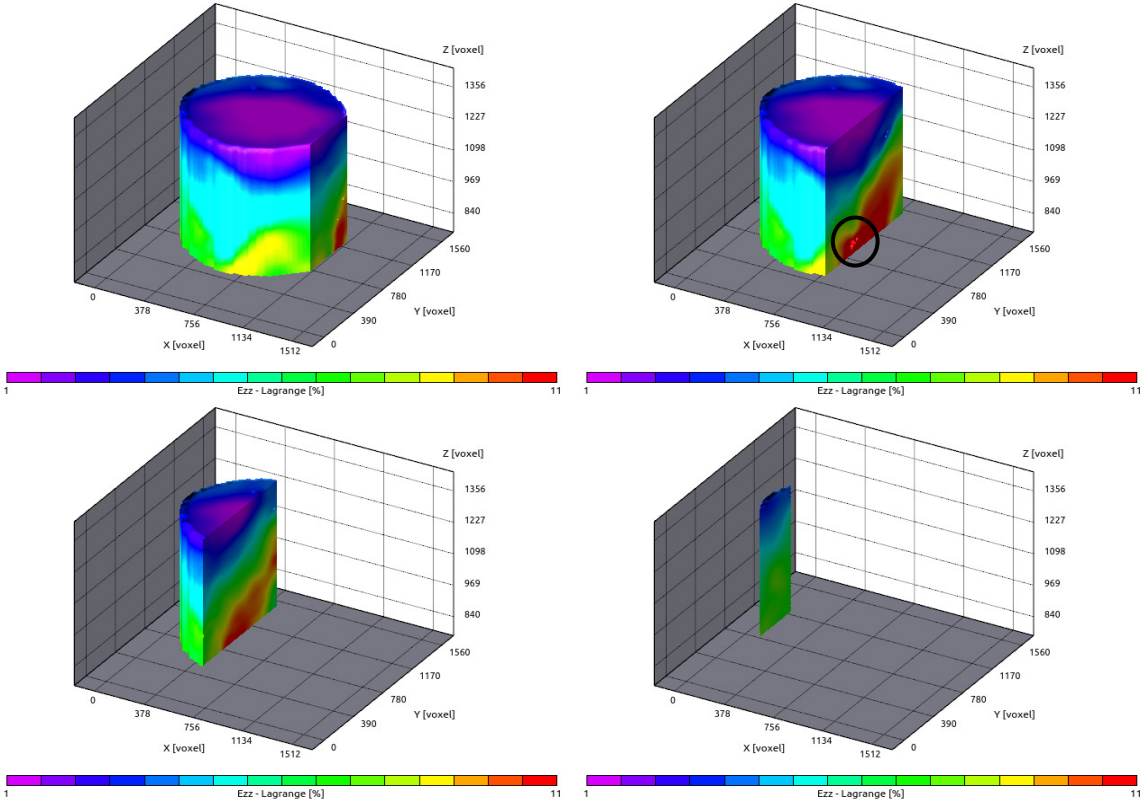


Figure 13: Strain field ϵ_{zz} correlated from the selected volumes in Figure 11 shown at different x-z planes.

4.4. Imperfections in the DVC Results

In section 4.2, we have seen that the image slice with low contrast and sparse features are non-ideal for DVC algorithm to calculate the displacement field. We then greatly improved the results by applying DVC to the enhanced tomography. The results are reasonable and they are consistent with the global loading that is applied to the specimen. However, if we examine through different planes inside the material body, we may still see some imperfections such as data drop-out as shown in the circled area in Figure 13. These imperfections may be caused by the poor contrast of the image, the few features in large volume or the artifacts in the tomography images. These are remaining challenges that need to be solved in the future.

5. CONCLUSIONS

In this feasibility study, we have applied DVC algorithm directly to the pre-existing tomography images from our previous in-situ XCT experiments of aluminum alloy 7075-T7351. We found out that DVC results from these original images had large errors and deviations due to its low-contrast and sparse features. However, we can greatly enhance the internal features/markers by thresholding the intensity of each image slice. DVC can then apply to these enhanced tomography images to obtain accurate displacement and strain results that are consistent with the global loading conditions applied to these specimens. It was proved that the internal features/markers inside the pre-existing tomography images can be suitable for DVC to calculate the deformation field if they were properly enhanced. The study shows that our original proposal to couple in-situ XCT experiments with DVC to calculate the deformation field throughout the material body is feasible, though there are quite a few challenges still ahead.

6. REFERENCES

1. Baruchel J, Buffiere JY, Maire E, Merle P, Peix G (2000) X-Ray Tomography in Material Science, Hermes Science Publications, ISBN: 2746291151.
2. Babout L, Ludwig L, Maire E, Buffiere JY (2003) Damage assessment in metallic structural materials using high resolution synchrotron X-ray tomography. Nucl Instrum Meth B 200: 303-07.
3. Maire E, Zhou, S, Adrien J, Dimichiel M (2011) Damage quantification in aluminum alloys using in situ tensile tests in X-ray tomography. Eng Frac Mech 78: 2679-90.
4. Morgeneyer TF, Starink MJ, Sinclair I (2008) Evolution of voids during ductile crack propagation in an aluminum alloy sheet toughness test studied by synchrotron radiation computed tomography. Act Mater 56: 1671-79.
5. Mota A, Jin H, Lu WY, Foulk JW, Johnson GC (2010) Quantifying the Debonding of Inclusions Through Tomography and Computational Homology, SAND2010-6646.
6. Jin H, Lu WY, Mota A, Foulk JW, Johnson GC, Korellis J (2013) A Study of Anisotropic Void Evolution in Aluminum Alloy using X-Ray Tomography. Exp Mech: DOI 10.1007/s11340-013-9765-y

DISTRIBUTION

1	MS 0555	E.C. Quintana, 1522
1	MS 0555	K.R. Thompson, 1522
1	MS 0557	D. Epp, 1522
1	MS 0557	D.G. Moore, 1522
1	MS 0840	J. M. Emery, 1524
1	MS 1139	T. J. Miller, 1535
1	MS 1139	P. L. Reu, 1535
1	MS 9042	M.E. Gonzales, 8250
1	MS 9042	B.R. Antoun, 8256
1	MS 9042	J.W. Foulk III, 8256
1	MS 9042	C. D. Moen, 8256
1	MS 9042	W.Y. Lu, 8256
1	MS 9042	T.J. Vogler, 8256
1	MS 9042	J. J. Dike, 8259
1	MS 9403	B. E. Mills, 8131
1	MS 9403	A. M. Morales, 8131
1	MS 9661	J. S. Korellis, 82541
1	MS 9957	H. Jin, 8256
1	MS 9957	A. Mota, 8256
1	MS 9957	B.T. Werner, 8256
1	MS 9957	J. A. Zimmerman, 8256
1	MS 0899	Technical Library, 8944 (electronic copy)
1	MS 0123	D. Chavez, LDRD Office, 1011



Sandia National Laboratories